# ON THE APPLICATION OF CTD TO THE FRACTURE MECHANICS

Y. Mitani* and H. Miyamoto**

## INTRODUCTION

The purpose of this paper is to combine the continuum theory of dislocations and conventional fracture mechanics, in order to clarify the physical aspects of deformation to seek a criterion of fracture from a microscopical point of view. These ideas were firstly realized by the BCS-Model [1], where one dimensional distribution of dislocations is assumed and the elastic-plastic -- problem is replaced by the problem of finding out an equilibrium distribution of dislocation under some suitable boundary conditions. Further progress has been made by Yokobori et al [2] and Lardner [3]. These direct applications of the BCS type solution, however, complicate the mathematical treatment, and seem to be inconvenient to the general plane problems. In this analysis the concept of dislocation theory is incorporated with Finite Element Method (FEM) to find out the equilibrium distribution of dislocations which satisfies the boundary conditions. It is noted that the estimation of the internal stress field due to the dislocation density is made fictitiously after Eshelby by self-consistent method [4] with the assumption that uniform plastic strain is produced by dislocation migration, if the dislocation were not confined in the elastic domain. The numerical analysis based on these fundamental concepts, (termed CTD hereafter) is carried out for monotonic loading condition, and the compatibility of the plastic deformation is examined for a centrally cracked plate.

## THEORETICAL FUNDAMENTALS AND NUMERICAL PROCEDURES

The equilibrium equation of BCS model may be rewritten, associated with a slip plane as:

$$\tau_a + \tau_{int} = \tau_c \ , \qquad (1)$$

in the plastic zone whose dimension appears as the integral limit of internal stress term $\tau_{int}$ as an unknown as well as the dislocation density - function. Here, $\tau_a$, $\tau_c$ denote the shear stress due to the external force and the frictional stress, respectively. The limitation of assuming the one-dimensional dislocation distribution will be overcome by properly estimating the internal stress field due to the dislocation and by examining the equation (1) in iterative fashion.

We assume the following mechanism for the calculation of the internal stress.

* National Institute of Technology, Mexico, D.F., Mexico.
** University of Tokyo, Tokyo, Japan.

(a) The plastic zone with uniform $\varepsilon_p$ in the elastic domain is represented by the surface forces after Eshelby

$$T_i = n_j \cdot c_{ijkl} \cdot \varepsilon^p{}_{kl} \ , \tag{2}$$

which are expressed by the nodal forces in FEM.

(b) The uniform plastic strain associated with the slip plane $\gamma^p$ is related with the excess dislocation density N with burgers vector b as

$$\gamma^p = (1/2)Nb \ , \tag{3}$$

where N is derived from the number of the equilibrium dislocation of BCS type solution for one-side pile-up [5] with a plane correction factor n*

$$N = \frac{\pi(1-\nu)n^*d}{\mu b} \cdot \tau_{eff} \ , \tag{4}$$

and

$$\tau_{eff} = (\tau_a + \tau_{int}) - \tau_c \ , \tag{5}$$

where $\tau_{int}$ vanishes for the initial stage.

Then we obtain the hardening ratio for uni-axial tension H' by considering $2\tau_c = \sigma_y$

$$H' = \frac{d\sigma}{d\varepsilon^p} = \frac{2}{\pi} \frac{\mu}{1-\nu} \frac{1}{n^* \cdot d} \ , \tag{6}$$

which shows the inverse proportional relation to the average grain diameter d. In this way we equivalently assumed the simple bilinear material characteristics by excess dislocation, and further discussions of dislocation distribution focus on the "geometrically necessary dislocation" after Ashby's terminology [6].

(c) Taking the irreversibility of plastic deformation into account, we obtain the internal stress field with free boundary condition for the specimenconfiguration. Hence the internal stress field is the sum of the stress due to the dislocation $\tau_d$ and its image stress $\tau_d^{im}$

$$\tau_{int} = \tau_d + \tau_d^{im} \ . \tag{7}$$

Hence, for each external stress increment, equation (7) is calculated by using relations (4), (3) and (2). Then equation (1) is examined until it holds. In the case of isotropic material, the slip plane is determined equal to the maximum shear plane of each incremental step.

The material constants used in this analysis are $E = 2.058 \times 10^{11}$ Pa, $\tau_c = 9.80$ MPa, $V = 0.333$, $b = 1.0$ A and $d = 10^{-6}$ m.





The specimen configuration is half width W/2 = 100, thickness B = 1.0 and half crack length a = 10 mm, respectively. The dislocation density VD and the total number of dislocation TND are defined in a yielded element as VD = N/d and TND = NA/d, respectively, where A is the area of the element in which stress and strain are defined as constant by FEM.

## RESULTS AND DISCUSSIONS

The typical feature obtained by this analysis is the bursting phenomena which depends highly on the plastic characteristics expressed by n*, that is, in the course of examination of equation (1), such loading stage appears where no convergence is obtained. It is seen in the divergence of TND in Figure 1, which implies that the compatible state can not exist and, hence the assumed condition (a) doesn't hold any more. Then it can be inferred that the excess dislocation which violate the compatibility might be emitted from the crack surface at this loading point, in order to recover the compatibility by the geometric change of the crack surface [7]. Since the effect of the internal stress field is highly localized near the crack tip, crack opening displacement increases non-linearly as shown in Figure 2, corresponding to the tendency of TND, where COD is plotted for the nearest joint of the crack tip.

These localized effect of the internal stress field influences also the spread of the plastic zone, and the resultant effects with the dislocation mobility show clearly the differences between the materials which have different n* as shown in Figures 3 and 4. It is noted that the bursting phenomena occur indifferent to the plastic zone size, instead, those materials which have n* smaller than 1.5, so far as this analysis is concerned, recover the stress singularity characteristics at the crack tip element is yielded before bursting occurs. This result implies the transition of fracture conditions according to the plastic property of the material from brittle to ductile. Figure 6 shows an example of stress singularity recovery after its relaxation.

Comparison is made in Figure 5 on plastic zone size. The discrepancy between the small scale yielding solution and the present analysis after the loading level around 0.4 presumably stems from the ignorance of the internal response due to the plastic deformation in s.s.y. analysis [8]. The difference to the BCS solution is due to the difference of the plastic zone dimension. The change of the internal state in terms of dislocation density distribution is clearly seen in Figure 7 which shows the difference of the equilibrium distributions not only by the amount but also by the position of the peak, where numbers in the Figure 7 denote those of the nearest elements around the crack tip from the front to the back.

From these facts we can conclude that s.s.y. concept is applicable to those materials which recover the stress singularity without violating the compatibility conditions and does not always mean the geometrical amount ratio to the other dimensions. The greater the n* is, the more easily the compatibility conditions is violated. Hence, for those materials which have smaller n* the conventional fracture criterion as the stress intensity factor might be applicable. In Table 1 the results are summarized, where NELM denotes the element number which has the maximum dislocation density just before the bursting occurs, and from which the excess dislocation might be emitted to the crack surface.

## CONCLUSIONS

The application of CTD to the elastic-plastic analysis is useful for discussing fracture phenomena for the following reasons:

(a) It analyses the compatibility of the plastic deformation which is responsible for the fracture in the case of nonhomogeneous deformation.

(b) The internal responses of the material or mechanisms can be discussed by the introduction of the concept of dislocation distribution which is ignored in the conventional fracture mechanics (especially in LFM).

The blunting phenomenon is explained by the emission of dislocations which violate the compatibility condition.

## ACKNOWLEDGEMENTS

One of the authors (Y. Mitani) expresses his heartiest gratitude to Professor E. Kröner of the University of Stuttgart for his valuable discussions and advice, and also to DAAD for their scholarship which enabled him to study in the above mentioned University. Their thanks are due to Dr. M. Kikuchi whose offer of FEM techniques and valuable discussions enabled the prompt completion of this work which is based on the dissertation of Y. Mitani at the University of Tokyo.

## REFERENCES

1. BILBY, B. A., COTTRELL, A. H. and SWINDEN, K. H., Proc. Roy. Soc. London, A272, 1963, 304.
2. YOKOBORI, T., YOSHIDA, M., KURODA, H., KAMEI, A. and KOUNOSU, S., Eng. Frac. Mech., 7, 1975, 377.
3. LARDNER, R. W., Proc. Roy. Soc. London, A317, 1970, 199.
4. ESHELBY, J. D., Solid State Phys., 3, Academic Press, New York, 1968, 79.
5. LOTHE, J. P. and HIRTH, J., "Theory of Dislocations", McGraw-Hill, New York, 1968, 704.
6. ASHBY, M. F., Phil. Mag., 21, 1970, 399.
7. KRONER, E., Private Communication.
8. RICE, J. R., Fracture 2, edited by H. Liebowitz, Academic Press, New York, 1969, 191.





Table 1 Bursting Stresses by Monotonic Loading for Different Correction Factor

| n* | Burst. Stress | TND | VD max. x $10^4$ | NELM | $\delta$ x $10^{-4}$ |
|---|---|---|---|---|---|
| 1.0 | - | - | - | - | - |
| 1.5 | 0.315 | 6767.83 | 74.76 | 1 | 0.9208 |
| 2.0 | 0.239 | 3634.25 | 24.68 | 1 | 0.8297 |
| 2.5 | 0.163 | 340.09 | 4.85 | 5 | 0.3914 |

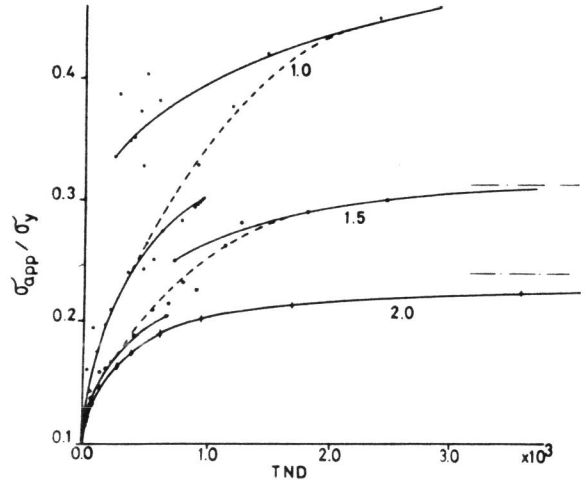


Figure 1 Variation of Total Number of Dislocation for Different Correction Factor

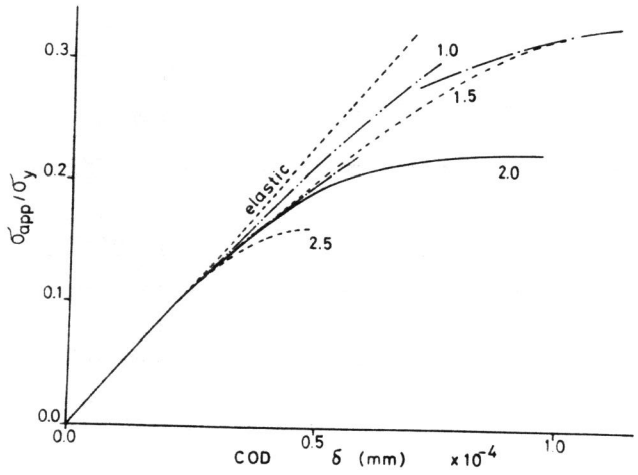


Figure 2 Variation of Crack Opening Displacement for Different Correction Factor

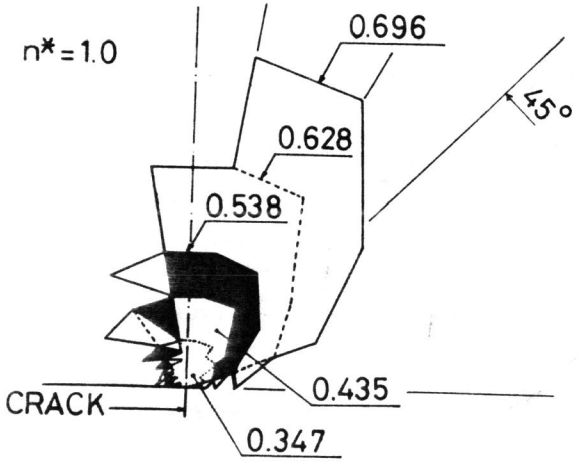


Figure 3 Spread of Plastic Zone for n* = 1.0





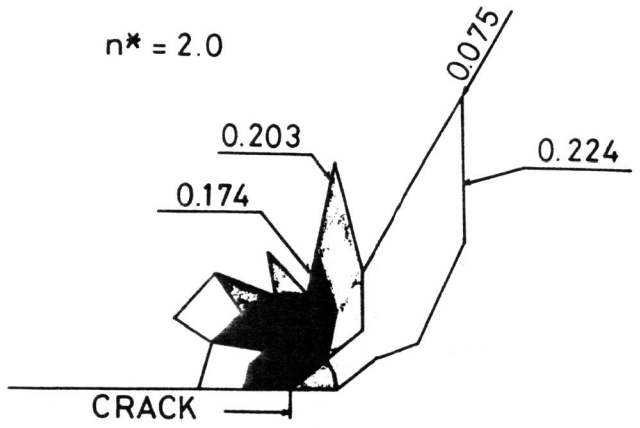


Figure 4 Spread of Plastic Zone for n* = 2.0

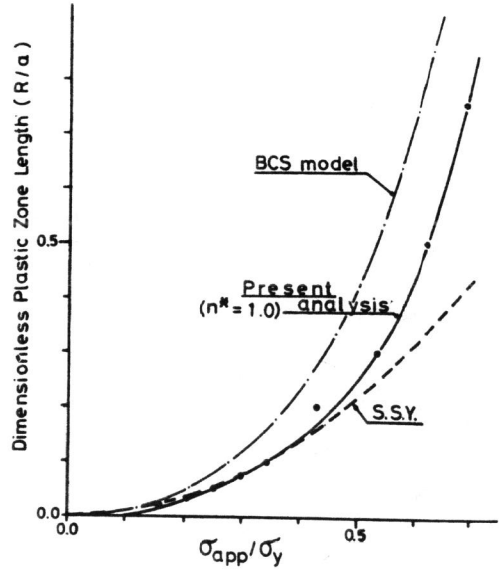


Figure 5 Comparison of Plastic Zone Length

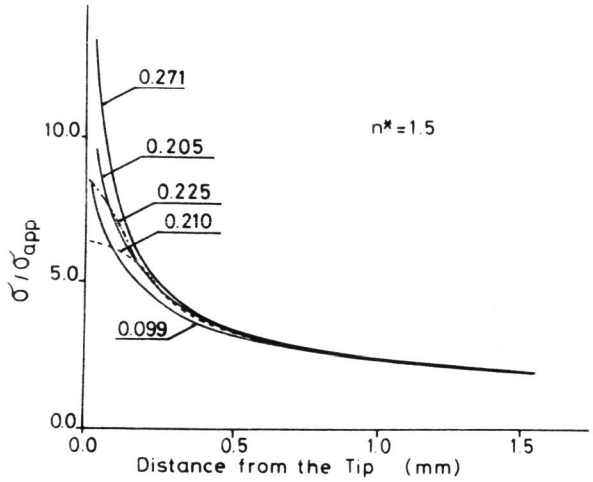


Figure 6 Variation of Stress Distribution Ahead of the Crack Tip for Different Loading Level

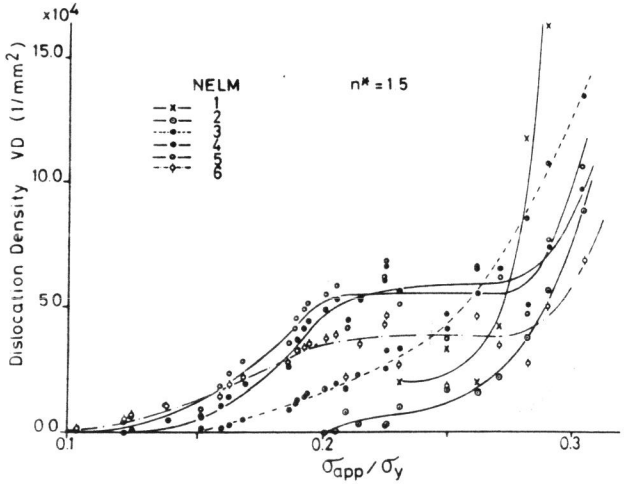


Figure 7 Variation of Dislocation Density Around the Crack Tip for n* = 1.5